Journal of Inflammation Research

Dovepress
Taylor & Francis Group

Open Access Full Text Article

ORIGINAL RESEARCH

Disulfidptosis-Induced Chondrocyte-Macrophage Crosstalk via GYS1/CCND1/NOD2 Axis Promotes Osteoarthritis Progression

Qing Sun[1,*], Zhihui Wei[1,*], Gaohai Shao[1], Mengfan Yang[1], Xianyan Zeng[2], Xiang Hong[1], Rong Gou[3], Han Zhang[4], Yining Zhang[5], Shuheng Dong[1], Yiming Qu[1], Yujiao Liu[1,5]

[1]Department of Orthopedics, Affiliated Yongchuan Hospital of Chongqing Medical University, Chongqing, 402160, People's Republic of China; [2]College of Pharmacy, Chongqing Medical University, Chongqing, 402160, People's Republic of China; [3]Affiliated Cancer Hospital of Chongqing University, Chongqing, 400000, People's Republic of China; [4]College of Biomedical Engineering, Hubei University of Medicine, Hubei, 442000, People's Republic of China; [5]Laboratory of Skeletal Development and Regeneration, Key Laboratory of Clinical Laboratory Diagnostics (Ministry of Education), College of Laboratory Medicine, Chongqing Medical University, Chongqing, 400016, People's Republic of China

*These authors contributed equally to this work

Correspondence: Yujiao Liu; Yiming Qu, Department of Orthopedics, Affiliated Yongchuan Hospital of Chongqing Medical University, Chongqing, 402160, People's Republic of China, Email 711878@hospital.cqmu.edu.cn; qim4786@126.com

Purpose: To investigate the potential role and underlying mechanisms of disulfidptosis, a novel form of regulated cell death, in the pathogenesis of degenerative osteoarthritis (OA), and to evaluate its association with M1-type macrophage infiltration and diagnostic biomarker potential.

Methods: Human articular cartilage samples from OA patients and non-OA controls were analyzed using high-throughput RNA sequencing to identify disulfidptosis-related gene expression patterns. Immunohistochemical assays were performed to validate key molecular signatures in chondrocytes. Differentially expressed genes (DEGs) were screened to identify candidates linking disulfidptosis to M1 macrophage biology. Functional correlation analyses were conducted to explore gene–immune cell interactions. Glucose starvation was applied to induce disulfidptosis in ATDC5 chondrocyte line; a co-culture system with RAW264.7 macrophage cell line was established to validate their functional roles and underlying mechanisms.

Results: OA chondrocytes exhibited a low-glucose metabolic state and elevated SLC7A11 (a cystine/glutamate transporter implicated in disulfidptosis) expression, consistent with a disulfidptosis signature, and showed increased immune infiltration of M1-type macrophages. Among the DEGs, Glycogen synthase 1 (GYS1) emerged as a key disulfidptosis-related gene directly regulating transcriptional programs in M1 macrophages. Functional analyses suggested that disulfidptosis in chondrocytes may indirectly promote M1 macrophage-mediated immune infiltration through cyclin D1 (CCND1) and nucleotide-binding oligomerization domain-containing protein 2 (NOD2), thereby contributing to OA progression.

Conclusion: Disulfidptosis in chondrocytes is associated with M1 macrophage immune infiltration and could drive OA progression. Mechanism genes like GYS1/CCND1/NOD2 have diagnostic potential and could be novel biomarkers and therapeutic targets for OA. These findings highlight the translational potential of targeting disulfidptosis-related pathways to improve OA management and patient outcomes.

Keywords: disulfidptosis, macrophages, osteoarthritis, GYS1, chondrocyte

Introduction

Degenerative Osteoarthritis (OA), an age-related joint disease characterized by progressive articular cartilage destruction, subchondral bone remodeling, and synovial inflammation, has become a major global public health challenge, affecting more than 300 million patients.[1] The disease not only causes joint pain and dysfunction, but also causes significant socioeconomic stress through direct medical expenditures, loss of labor, and family care burden, especially in aging societies.[2] Current treatment strategies (such as analgesics, nonsteroidal anti-inflammatory drugs, articular injections of

https://doi.org/10.2147/JIR.S568766
Received: 25 September 2025
Accepted: 21 December 2025
Published: 6 January 2026

Graphical Abstract

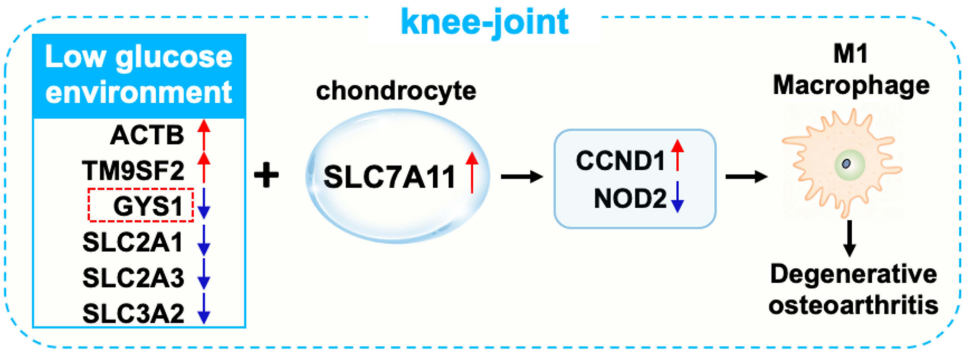

hyaluronic acid, and total joint replacement) are primarily targeted at symptom relief, do not interrupt disease progression, and long-term efficacy is severely limited by drug toxicity, surgical complications, and a high recurrence rate.[3] At present, disease-modifying drugs targeting the core pathological mechanisms of OA, including abnormal chondrocyte metabolism, inflammatory factor cascade and dysregulation of mechanical signaling, are still lacking, which highlights the urgent need to develop novel therapeutic strategies based on multi-target regulation.

Disulfidptosis is a novel type of regulated cell death driven by the toxic accumulation of disulfide bonds and subsequent cytoskeletal collapse under metabolic stress conditions. It was first discovered by the team of Prof. Boyi Gan and Junjie Chen at MD Anderson Cancer Center in 2023.[4] This mode of cell death is due to the high expression of SLC7A11 (member 11 of the solute carrier family, also known as xCT) under the condition of glucose starvation, resulting in insufficient intracellular NADPH (reduced nicotinamide adenine dinucleotide phosphate) supply, abnormal accumulation of cystine and other disulfide, and destruction of the structure of cytoskeletal proteins (such as actin), which triggers cell death. Disulfidptosis contributes to the pathogenesis of diverse diseases, including cancer,[4] neurodegenerative disorders,[5–8] and liver conditions.[9–11] Recent bioinformatics analyses have further implicated disulfidptosis-related genes in OA progression and diagnosis,[12–15] suggesting its potential role as a core pathological mechanism.

OA is not only a mechanical degenerative disorder but also accompanied by significant immunological alterations. The infiltration and activation of immune cells, particularly macrophages, within the synovium and articular cartilage are pivotal drivers of chronic inflammation, matrix degradation, and pain, thereby accelerating OA progression.[16] At the cellular level, pathogenic mechanisms such as oxidative stress, mitochondrial dysfunction, and impaired autophagy—all linked to redox imbalance—contribute directly to chondrocyte death and dysfunction.[17] Emerging as a novel redox-related cell death modality, disulfidptosis has been implicated in the pathogenesis of various cancers,[18–20] vascular,[21] and neurological diseases,[5] where it actively shapes the immune microenvironment.[22] For instance, disulfidptosis can regulate the exhaustion of tumor-infiltrating CD8 T cells, demonstrating its intrinsic capacity to modulate immune cell fate and function.[23] However, the precise functional mechanisms and regulatory networks by which disulfidptosis in chondrocytes contributes to OA pathogenesis through immune cell infiltration remain incompletely characterized, hindering its translational potential.

Therefore, the development of disease-modifying drugs targeting the core pathological mechanisms of OA remains an area requiring further exploration. In this study (Figure 1: analysis process), by integrating clinical cartilage samples with high-throughput sequencing data, we systematically characterized gene expression in articular chondrocytes from OA patients, aiming to uncover its potential relationship with disulfidptosis. Furthermore, we investigated the interaction between immune cell infiltration and disulfidptosis. This integrated multi-omics analytical approach will provide new perspectives for understanding the molecular mechanisms of OA. Critically, by defining the key genes (eg, *GYS1, CCND1, NOD2*) within this network, GYS1 downregulation has been associated with impaired glucose metabolism in

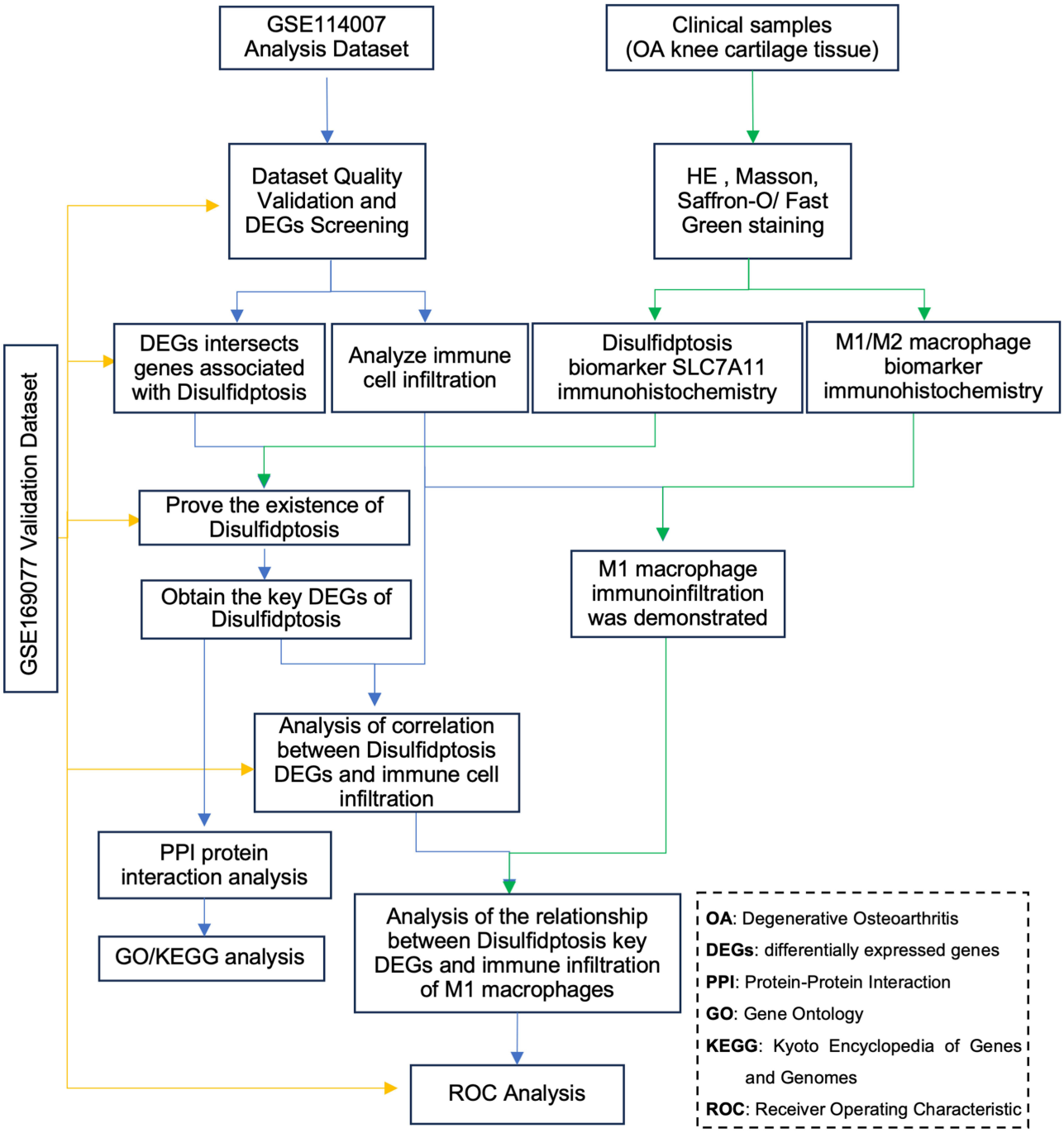

Figure 1 Chart of Overall Project Analysis.

OA chondrocytes,[24] while CCND1 overexpression promotes synovial inflammation[25]-suggesting potential crosstalk between these pathways. Our work not only elucidates a novel pathogenic mechanism but also pinpoints potential diagnostic biomarkers and therapeutic targets for developing novel disease-modifying strategies.

Materials and Methods

Reagents and Consumables

The ATDC5 (mouse chondrogenic cell line) and RAW264.7 (mouse monocytic macrophage cell line) were obtained from the European Collection of Authenticated Cell Cultures (ECACC) and the American Type Culture Collection (ATCC),

https://doi.org/10.2147/JIR.S568766

respectively, and maintained in DMEM (Gibco, USA) supplemented with 10% FBS (Wisent, Canada) at 37 °C with 5% CO_2. Glucose-free DMEM was purchased from Bio-channel (Nanjing, China), dithiothreitol (DTT) from MedChemExpress (NJ, USA), and the actin ring staining kit (YF 488-Phalloidin) from UElandy (Suzhou, China). Hematoxylin and eosin (HE) staining solution was purchased from Beyotime Biotechnology Co., LTD (Shanghai, China). Saffron-O/ Fast green cartilage staining and Masson staining kit were purchased from Beijing Solarbio Science & Technology Co., Ltd (Beijing, China). xCT antibody, GLUT1 antibody, CD86 antibody, CD206 antibody and HRP labeled Rabbit IgG (H+L) were purchased from Affinity Bioscience (OH, USA), immunohistochemical dilution ratios were 1:100, 1:100, 1:200, 1:200 and 1:500, respectively. DAB (diaminobenzidine) color developing kit is purchased from Beijing Zhong Shan-Golden Bridge Biological Technology CO., LTD (Beijing, China).

Data Download and Standardization

Gene Expression Omnibus (GEO) is a public repository hosting functional genomic datasets. We obtained the RNA sequencing dataset (accessed in December 2024) GSE114007, which contains sequencing data from 10 normal and 10 OA human articular cartilage samples based on platform GPL18573. Additionally, dataset GSE169077 was downloaded as a validation set, comprising 5 normal and 6 OA cartilage samples. The use of these de-identified, publicly available datasets for secondary analysis was reviewed and approved by the Ethics Committee of Chongqing Medical University Affiliated Yongchuan Hospital (Approval No.: 2024EC0074), confirming compliance with ethical standards.

To ensure data quality and consistency, we preprocessed the datasets using R software (version 4.3.3) by applying a log2(x+1) transformation to reduce skewness and improve normality, followed by Z-score normalization. Data distribution and normalization effects were visualized using box plots, while inter-group structural differences were assessed through Principal Component Analysis (PCA).

Clinical Samples Collection

Articular cartilage specimens were collected from 20 knee OA patients (Kellgren-Lawrence Grade 4; age 64.9±6.2 years; 4 males/16 females) undergoing total knee arthroplasty. Patients fulfilled clinical OA diagnostic criteria and were excluded for coexisting joint diseases or prior medication exposure. Using published protocols,[26] samples were obtained from two anatomical regions of the same joint: the relatively preserved cartilage distal to the major wear regions (stage I), which was histologically confirmed to exhibit no signs of OA-like changes (eg, surface fibrillation or proteoglycan loss), served as the internal-control group; the erosion-adjacent cartilage with subchondral bone exposure (stage IV) served as the OA group. All specimens were snap-frozen in liquid nitrogen immediately after collection and subsequently transferred to −80°C freezers for cryopreservation to minimize degradation, with all samples processed uniformly at the same time using identical methods.

The sample size for this paired-sample study (n=20 pairs) was not based on conventional power calculation for group comparisons, but rather on the feasibility of obtaining matched, high-quality tissue specimens from the same patient. This matched-pairs design, where each OA specimen is compared to its own internal control from the same joint, dramatically reduces inter-individual biological variability (eg, genetic background, age, sex, comorbidities, and overall joint micro-environment). This control for confounding factors significantly increases the statistical sensitivity and power to detect true biological differences compared to unpaired designs, which often require much larger sample sizes to achieve equivalent confidence.

The study complies with the Declaration of Helsinki, and received ethical approval (Yongchuan Hospital Ethics Committee #2024EC0074; Chinese Clinical Trial Registry ChiCTR2500097743), with written informed consent obtained preoperatively.

Hematoxylin and Eosin (HE) Staining

Cartilage tissues from distinct zones were excised en bloc with subchondral bone using rongeurs. Specimens were fixed in 4% paraformaldehyde for 24 hours followed by 14% EDTA decalcification for approximately two weeks. Subsequent processing included sequential dehydration through graded ethanol series (75%-80%-95%-100%-100%, 2 hours per concentration), paraffin infiltration, and oriented embedding with the cartilage-bone interface facing downward to ensure

simultaneous visualization of both tissues in sections. Serial 5-μm sections were prepared using a Leica microtome. HE staining was performed as previously described:[27] Sections were baked at 62°C for 2 hours, dewaxed in xylene I/II (1 hour each), and rehydrated through graded ethanol (100%-95%-80%-70%, 3 minutes each) to ddH_2O. Nuclear staining with hematoxylin (3 minutes) was followed by 1% acid-alcohol differentiation (1–2 seconds), bluing in saturated lithium carbonate (1–2 seconds), and cytoplasmic counterstaining with eosin (5 minutes). Dehydration through reverse ethanol gradients and neutral resin mounting completed the protocol.

Saffron-O/Fast Green Cartilage Staining

Following the same dewaxing and rehydration procedures as HE staining, tissue sections were processed according to the staining kit protocol: Sections were stained with Weigert's solution for 5 minutes, differentiated in acid solution for 15 seconds, counterstained with Fast Green for 5 minutes, briefly rinsed with weak acid solution (15 seconds), then immersed in saffron O solution for 5 minutes. Finally, sections were dehydrated through graded ethanol series and mounted with neutral resin.

Masson Staining

Following dewaxing and rehydration, tissue sections were processed per the staining kit protocol: Sections were stained with Weigert's iron hematoxylin for 5 minutes, differentiated in acid-alcohol solution for 5 seconds, then blued in Masson bluing solution. Subsequent counterstaining included 5 minutes in Ponceau-fuchsin solution and 1 minute in aniline blue solution, with intermittent rinses using weak acid working solution. Finally, sections were dehydrated through a graded ethanol series and permanently mounted.

Immunohistochemistry

Immunohistochemical staining was performed as previously described.[26] Briefly, dewaxed and rehydrated sections were treated with 3% H_2O_2 to block endogenous peroxidase activity. Antigen retrieval was achieved by 0.05% trypsin digestion at 37°C for 40 minutes, followed by 10% goat serum blocking. Sections were incubated with mouse polyclonal primary antibody overnight at 4°C, then with HRP-conjugated rabbit anti-mouse IgG (H+L) secondary antibody at room temperature for 40 minutes. DAB chromogen development was monitored microscopically, with brown-yellow granular deposits indicating positive staining. Sections were counterstained with hematoxylin, blued, and mounted for observation. Non-immune IgG served as negative controls.

Considering the significant difference in chondrocyte density between stage I and stage IV articular cartilage, three representative fields per region per sample were evaluated in a blinded manner. The mean percentage of positive cells (positive cells / total cells) was used for statistical comparison. Data were presented using paired data plots with connecting lines. Statistical differences between paired groups were determined using a paired *t*-test.

Screening and Visualization of Differentially Expressed Genes (DEGs)

For identification of DEGs between groups, we employed *t*-test using the limma package in R to calculate p-values and log2 fold changes (log2FC). DEGs were screened at a significance threshold of $p < 0.05$ and $|log2FC| > 0.585$ (equivalent to fold change >1.5). Venn diagrams and volcano plots were generated using the ggplot2 package to visualize the DEGs.

Screening and Visualization of Phenotypic Related Differential Genes

Through Genecards (https://www.genecards.org/) download phenotypic correlation gene set a public database, by Wayne figure analysis dataset difference gene related to phenotype of overlap, and through the ggplot2 package map genetic variations of Heatmaps and expression of cellular.

Construction of Protein-Protein Interaction (PPI) Networks

Based on differentially expressed genes, a PPI network was constructed using the STRING database with the minimum required interaction score of 0.7 (highest confidence level). The network was visualized using the igraph package, and

hub proteins were screened based on degree centrality metric. This PPI network analysis elucidated functional interactions among these critical differentially expressed genes.

Immune Infiltration and Correlation Analysis

The ssGSEA (single sample Gene Set Enrichment Analysis) algorithm from the R package "GSVA" was employed to quantify immune cell infiltration levels. This method calculates enrichment scores for each immune cell type in samples based on cell-specific marker gene sets.[28] Pearson correlation analysis was performed to assess statistical relationships between key DEGs and immune cell infiltration scores. Results were visualized through Heatmaps and correlation scatter plots to illustrate associations between candidate genes and distinct immune cell subtypes.

LASSO Regression Analysis

LASSO regression is a regularization method that can effectively reduce the complexity of a model and select variables of importance. Through the "glmnet" package of R software, LASSO regression model was applied to calculate the LASSO coefficients of differential genes, and the best regularization parameters were determined by cross-validation. A variable with a non-zero coefficient is considered to have a significant association with the target variable. At the same time, the trajectory diagram of LASSO variables was drawn to observe the selection of variables under different λ values. Variables with small correlation whose coefficients quickly become zero during the increase of λ were excluded, and genes with high correlation were screened.

Cell Culture and Treatments

ATDC5 cells were seeded in 24-well plates at a density of 1×10^4 cells per well. After attachment, the culture medium was replaced with one of the following: complete DMEM, glucose-free DMEM, or glucose-free DMEM supplemented with 0.5 mM DTT.[29] Cells were cultured for 12 hours and then either fixed with 4% paraformaldehyde for actin ring staining,[30] lysed with TRIzol reagent (Thermo Fisher Scientific, Massachusetts, USA) for RNA extraction, or co-cultured with RAW264.7 cells at a 1:4 ratio[27,30] for an additional 12 hours prior to RNA extraction. RT-qPCR was performed as previously described.[30] Gene-specific primers are listed in Table S1.

Receiver Operating Characteristics (ROC) Analysis

The ROC curve analysis is a well-established method to evaluate the capability of biomarkers in discriminating individuals with disease progression from unaffected controls. This approach was applied to assess the predictive power of screened key DEGs in distinguishing sample groups. Using the pROC package in R, the area under the curve (AUC) values were calculated to validate model reliability and sensitivity, where AUC values approaching 1 indicate superior discriminative performance. ROC curves were graphically visualized to evaluate the diagnostic potential of candidate genes under disulfidptosis-related conditions.

Statistical Analysis

Data were analyzed using GraphPad Prism 8.3. Pairwise comparisons were conducted using Student's *t*-test, while comparisons among three groups with a single independent variable were assessed by one-way ANOVA. A (p)-value < 0.05 was considered statistically significant.

Results

Transcriptomic Profiling Identifies Disulfidptosis-Associated Genes in Osteoarthritic Cartilage

Processed RNA-seq data (GSE114007) from degenerative arthritis cartilage samples underwent quality control and normalization. Box plots confirmed data standardization efficacy (Figure 2A). PCA revealed significant transcriptomic divergence between OA (n=10) and control (n=10) cohorts (Figure 2B). Differential expression analysis identified 5341

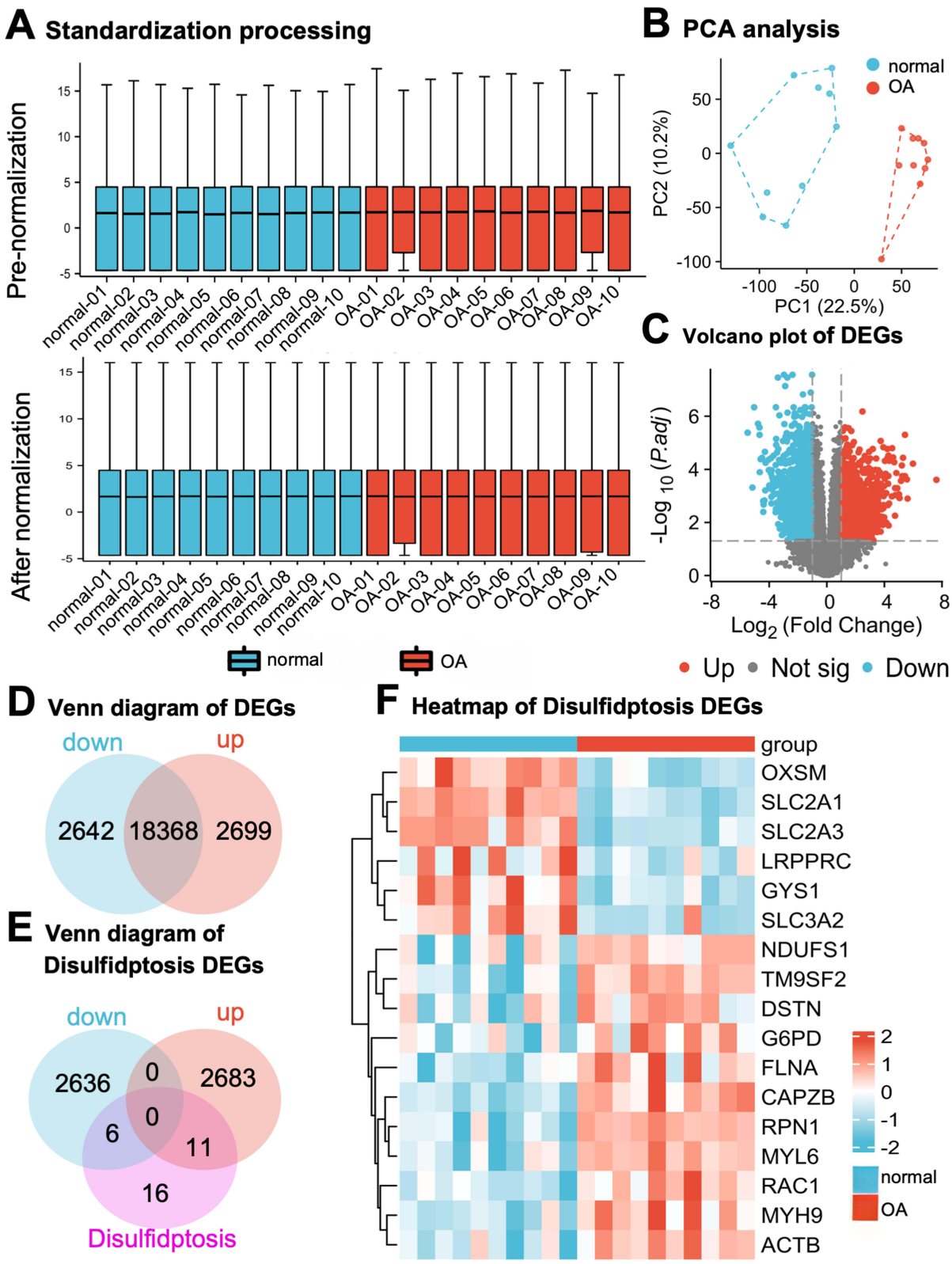

Figure 2 Transcriptomic Profiling Identifies Disulfidptosis-Associated Genes in Osteoarthritic Cartilage. (**A**) Comparison of data quality box drawing before and after standardization. (**B**) Principal component analysis of differential genes in OA sample and control group. (**C**) Volcano plot showed significantly expressed genes. (**D**) Venn diagram screened the differential genes. (**E**) Venn diagram showed the differential genes associated with disulfidptosis. (**F**) Heatmap showed 17 DEGs associated with disulfidptosis.

https://doi.org/10.2147/JIR.S568766

DEGs (including 2699 up-regulated genes and 2642 down-regulated genes), visualized by volcano and Venn plots (Figure 2C and D).

Intersection analysis of DEGs with 33 disulfidptosis-related genes (from Genecards) yielded 17 disulfidptosis-linked DEGs, 11 of which were up-regulated and 6 of which were down-regulated (Figure 2E and F). Among them, the proteins encoded by *SLC2A1, SLC2A3, OXSM, GYS1, SLC3A2, RPN1, G6PD* and *RAC1* are key proteins in glucose metabolism and transport, while *CAPZB, MYH9, MYL6, ACTB* and *FLNA* are key genes in cytoskeleton formation and regulation. These are important regulatory factors leading to the occurrence of disulfidptosis, which is characterized by disulfide stress caused by excessive intracellular cystine accumulation in the absence of glucose, leading to abnormal remodeling of the actin cytoskeleton and cell death. These gene changes indicate that there are glucose metabolism changes and cytoskeletal remodeling abnormalities in articular cartilage tissue of OA patients, and there may be disulfidptosis.

Histopathological and Immunohistochemical Validation of Disulfidptosis in Human OA Cartilage

Histopathological examination of osteoarthritic cartilage revealed progressive structural and compositional deterioration. Sectional samples from knee replacement patients (Figure 3A) demonstrated marked differences between stage I and stage IV regions. Stage I displayed intact cartilage architecture with a smooth surface, tightly organized extracellular matrix, and evenly distributed chondrocytes exhibiting typical rounded morphology with prominent nuclei (Figure 3B). In contrast, stage IV showed substantial surface erosion with fissures and focal detachment, accompanied by significant hypocellularity and cellular abnormalities including chondrocyte hypertrophy, nuclear enlargement, and disorganized arrangement.

Special staining techniques confirmed progressive matrix degradation in diseased cartilage. Saffron-O/ Fast Green staining revealed abundant glycosaminoglycan content (intense red) and well-organized superficial collagen (green) in stage I. stage IV exhibited markedly diminished Saffron O staining indicating proteoglycan loss, alongside expanded and disorganized Fast green staining suggesting collagen fiber disarray (Figure 3C). Masson's trichrome staining further demonstrated intact, uniformly blue-stained type II collagen networks in stage I, while stage IV showed attenuated blue staining with appearance of red-stained type I collagen in eroded areas, indicating collagen matrix degeneration (Figure 3D).

Immunohistochemical analysis identified molecular evidence of disulfidptosis in advanced OA. xCT protein expression, encoded by *SLC7A11* and responsible for cystine/glutamate transport, was significantly elevated in stage IV chondrocytes compared to stage I in 75% of patients (Figure 3E and S1). This overexpression of the cystine transporter under conditions of nutrient stress supports the potential activation of disulfidptosis pathways in severely damaged OA cartilage.

Disulfidptosis-Associated Genes Are Linked to Dysregulated Glucose Transport and Metabolism

Analysis of the independent validation dataset GSE169077 confirmed the involvement of disulfidptosis-related pathways in osteoarthritis. Standardized processing and quality control were performed (Figure S2A), with PCA demonstrating clear separation between OA and control samples (Figure S2B). Differential expression analysis identified 765 DEGs, 314 upregulated and 451 downregulated (Figure S2C and 4A). Intersection with 33 disulfidptosis-related genes revealed 6 significant overlaps (Figure 4B and C), all of which were consistently dysregulated in the primary GSE114007 dataset (Figure 4D). Specifically, *ACTB* and *TM9SF2* were upregulated, while *GYS1, SLC2A1, SLC2A3* and *SLC3A2* were downregulated (Figure 4E and F).

PPI analysis demonstrated strong functional connectivity among five of these proteins (excluding TM9SF2) (Figure 4G). GO and KEGG enrichment analyses of these core genes revealed significant enrichment in glucose-related processes and pathways (Figure 5). Analysis of the top 10 significantly enriched terms revealed that GO Biological Processes (BP) included glucose import, while Molecular Functions (MF) encompassed glucose binding, D-glucose transmembrane transporter activity, organic anion transmembrane transporter activity, glucose transmembrane

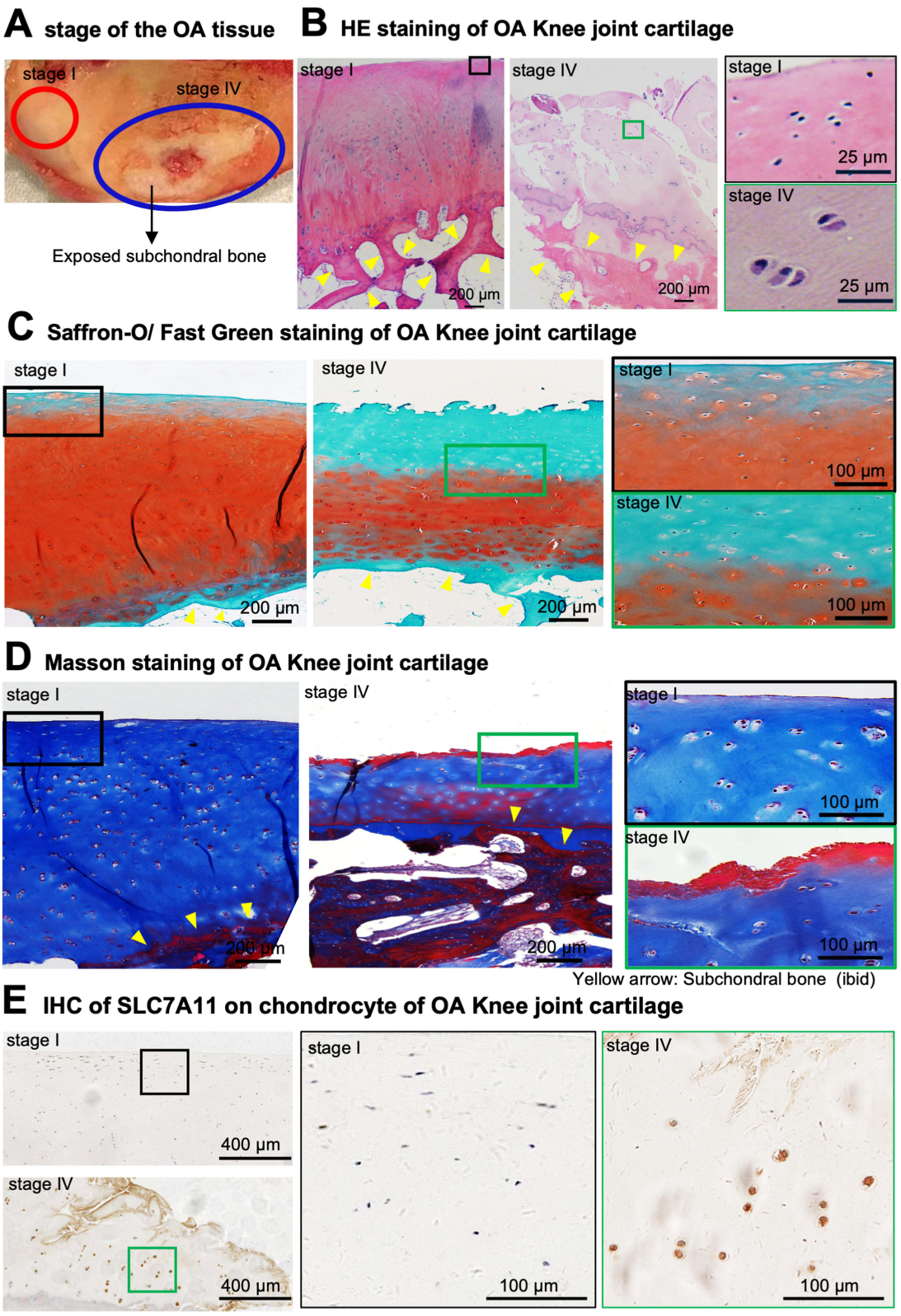

Figure 3 Histopathological and Immunohistochemical Validation of Disulfidptosis in Human OA Cartilage. (**A**) Zonal classification of knee joint tissue samples (stage I vs IV). The red and blue ovals indicate the sampling sites for stage I and stage IV, respectively. (**B**) HE staining. (**C**) saffron O/ Fast green staining. (**D**) Masson staining. (**E**) Immunohistochemical staining for xCT (SLC7A11-Encoded Protein). The yellow arrows highlight the subchondral bone. The higher-magnification images with black and green borders on the right correspond to the areas enclosed by the black and green rectangles in the lower-magnification image on the left.

https://doi.org/10.2147/JIR.S568766

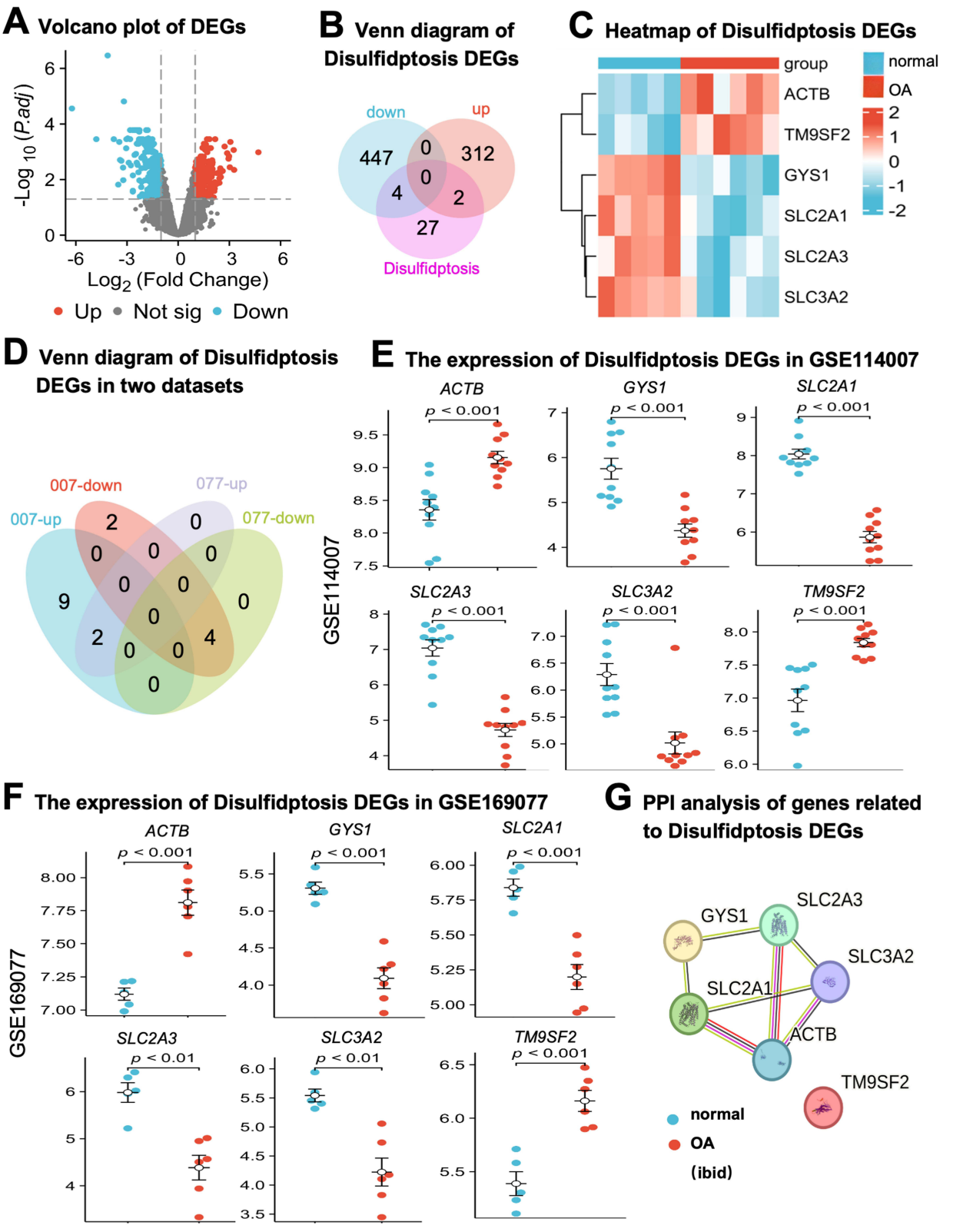

Figure 4 Disulfidptosis-associated differential genes are functionally linked to glucose transport. (**A**) Volcano plot of DEGs (OA vs controls). (**B**) Venn diagram identifying six disulfidptosis-associated genes. (**C**) Heatmap of differentially expressed genes. (**D**) Venn diagram of DEGs in GSE114007 and GSE169077 datasets. (**E** and **F**) Scatter plots showing expression trends of DEGs in (**E**) GSE114007 and (**F**) GSE169077 datasets. (**G**) PPI network of DEGs.

https://doi.org/10.2147/JIR.S568766

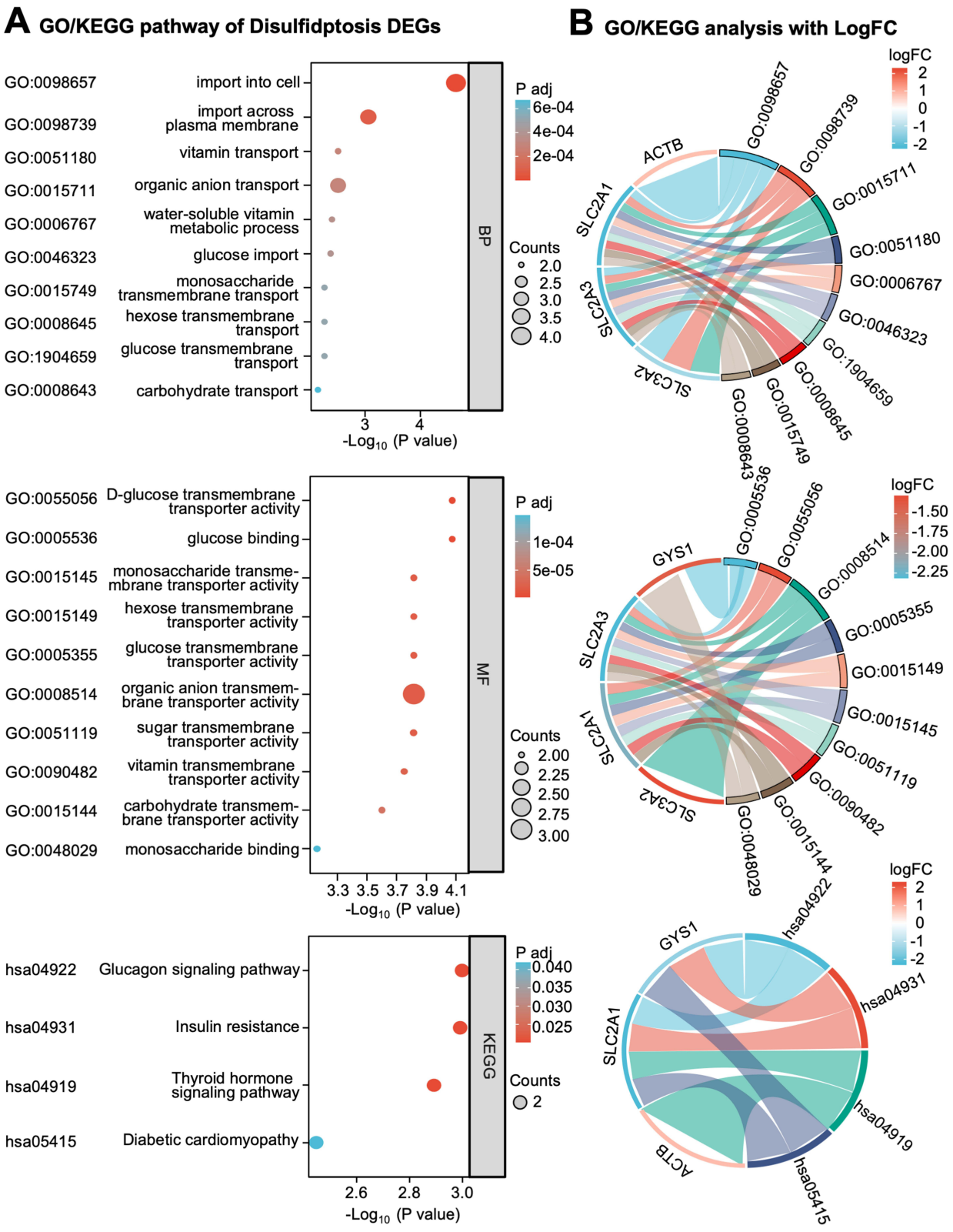

Figure 5 Disulfidptosis-Associated Genes Are Linked to Dysregulated Glucose Transport and Metabolism. (**A**) Bubble plot of GO and KEGG functional enrichment analysis. (**B**) Chord diagram integrating GO/KEGG terms with log2FC values in the GSE169077 dataset.

https://doi.org/10.2147/JIR.S568766

transporter activity, hexose transmembrane transporter activity, monosaccharide transmembrane transporter activity, sugar transmembrane transporter activity, vitamin transmembrane transporter activity, carbohydrate transmembrane transporter activity, and anion transmembrane transporter activity. KEGG pathways included Glucagon signaling pathway, Insulin resistance, Thyroid hormone signaling pathway, and Diabetic cardiomyopathy, all of which are closely associated with glucose metabolism. Notably, 85% of enriched BP and MF terms related to energy transport, with 35.3% specifically involving sugar transport mechanisms. These results strongly suggest that disulfidptosis in OA chondrocytes may be mediated through dysregulation of glucose transport processes.

Disulfidptosis-Related Genes Modulate Overall Immune Infiltration Landscapes in OA

Studies have shown that OA is not just a mechanical disease, but that changes in the immune system may also play an important role in its pathogenesis. Immune cell infiltration analysis of the GSE114007 dataset using established gene signatures[28] revealed significantly altered infiltration levels in osteoarthritic cartilage for the following cell types: CD8 T cells, cytotoxic cells, dendritic cells (DC), eosinophils, macrophages, mast cells, Th17 cells, Th2 cells, and regulatory T cells (Treg) (Figure 6A and B). GSE169077 dataset demonstrated markedly elevated infiltration of CD8 T cells, macrophages, NK cells (Figure 6C and D). This multi-dataset analysis establishes CD8 T cells and macrophages as predominant immune populations mechanistically linked to osteoarthritis pathogenesis.

Furthermore, we analyzed the correlation between 6 disulfidptosis-related DEGs and two types of immune cells across two datasets. The correlation Heatmap (Figure S3) and scatter plots (Figure 6E and S4) revealed that *ACTB* and *TM9SF2* expression levels showed significant negative correlations with CD8 T cell infiltration but positive correlations with macrophage infiltration. Conversely, *CYS1, SLC2A1*, and *SLC2A3* expression demonstrated significant positive correlations with CD8 T cell infiltration and negative correlations with macrophage infiltration. Integrated analysis indicated that the co-expression pattern of these disulfidptosis-related DEGs—characterized by elevated *ACTB* and *TM9SF2* alongside reduced *CYS1, SLC2A1*, and *SLC2A3*—was associated with an immune microenvironment skewed toward increased macrophage infiltration and decreased CD8 T cell infiltration.

GYS1-Mediated Disulfidptosis Drives M1 Macrophage Polarization in the Osteoarthritic Niche

Macrophage-mediated immune infiltration, particularly M1 polarization, significantly contributes to degenerative arthritis pathogenesis. Enzymes secreted by M1 macrophages, such as matrix metalloproteinases (MMPs), break down the cartilage matrix, thereby degrading the cartilage and promoting the occurrence of degenerative changes.[31] Immunohistochemical analysis of human articular cartilage demonstrated elevated CD86 (M1 marker) expression and diminished CD206 (M2 marker) expression in severely damaged stage IV compared to intact stage I (Figure 7A), indicating M1 macrophage accumulation in diseased regions. Integration of M1 macrophage phenotype-related genes from Genecards with GSE114007 DEGs yielded 18 candidates (Figure 7B and C). Subsequent random forest (Figure 7D) and LASSO regression analyses (Figure 7E and F) identified eight core regulators: *NOD2, EXPH5, IGF2BP2, MIR155HG, CCND1, FN1, DEPDC1*, and *ITGB2*.

Regrouping GSE114007 based on disulfidptosis gene expression (*SLC2A1/SLC2A3/GYS1/ACTB*) revealed distinct DEGs profiles (Figure S5A). Cross-analysis of these groups with M1-associated genes identified 23 common targets (Figure 8A). Further intersection with the LASSO-derived eight-gene set pinpointed three key mediators: *CCND1, ITGB2*, and *NOD2* (Figure 8B and C). Expression validation in GSE114007 demonstrated that while *ITGB2* expression was negatively correlated with *SLC2A1* expression (Figure 8D), inconsistent with the grouping results (Figure 8C, right), *CCND1* and *NOD2* expressions showed significant negative and positive correlations with *GYS1*, respectively (Figure 8D), consistent with grouping analyses (Figure 8C, left). This establishes GYS1 as a central regulator of M1 macrophage infiltration genes, potentially exacerbating OA progression via CCND1 and NOD2 signaling.

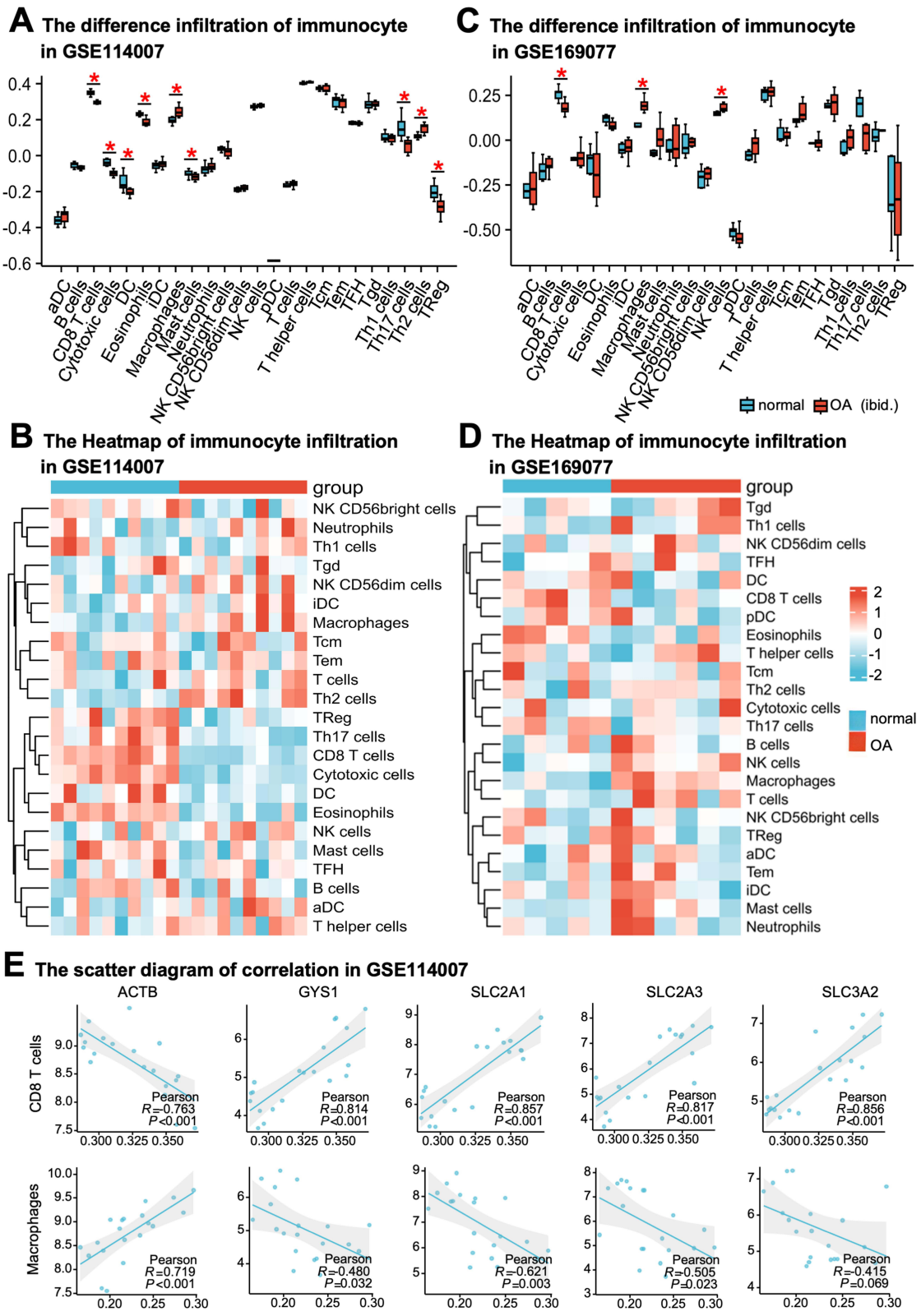

Figure 6 Osteoarthritic articular cartilage exhibits immune cell infiltration. (**A**) Comparative box plots of immune cell infiltration in the GSE114007 dataset. (**B**) Heatmap of immune-related gene expression in GSE114007 dataset. (**C**) Comparative box plots of immune cell infiltration in the GSE169077 dataset. (**D**) Heatmap of immune-related gene expression in GSE169077 dataset. (**E**) Correlation scatter plots of disulfidptosis-associated DEGs and immune cells in GSE114007 datasets. *p < 0.05 vs normal by *t*-test for panels (**A** and **C**).

https://doi.org/10.2147/JIR.S568766

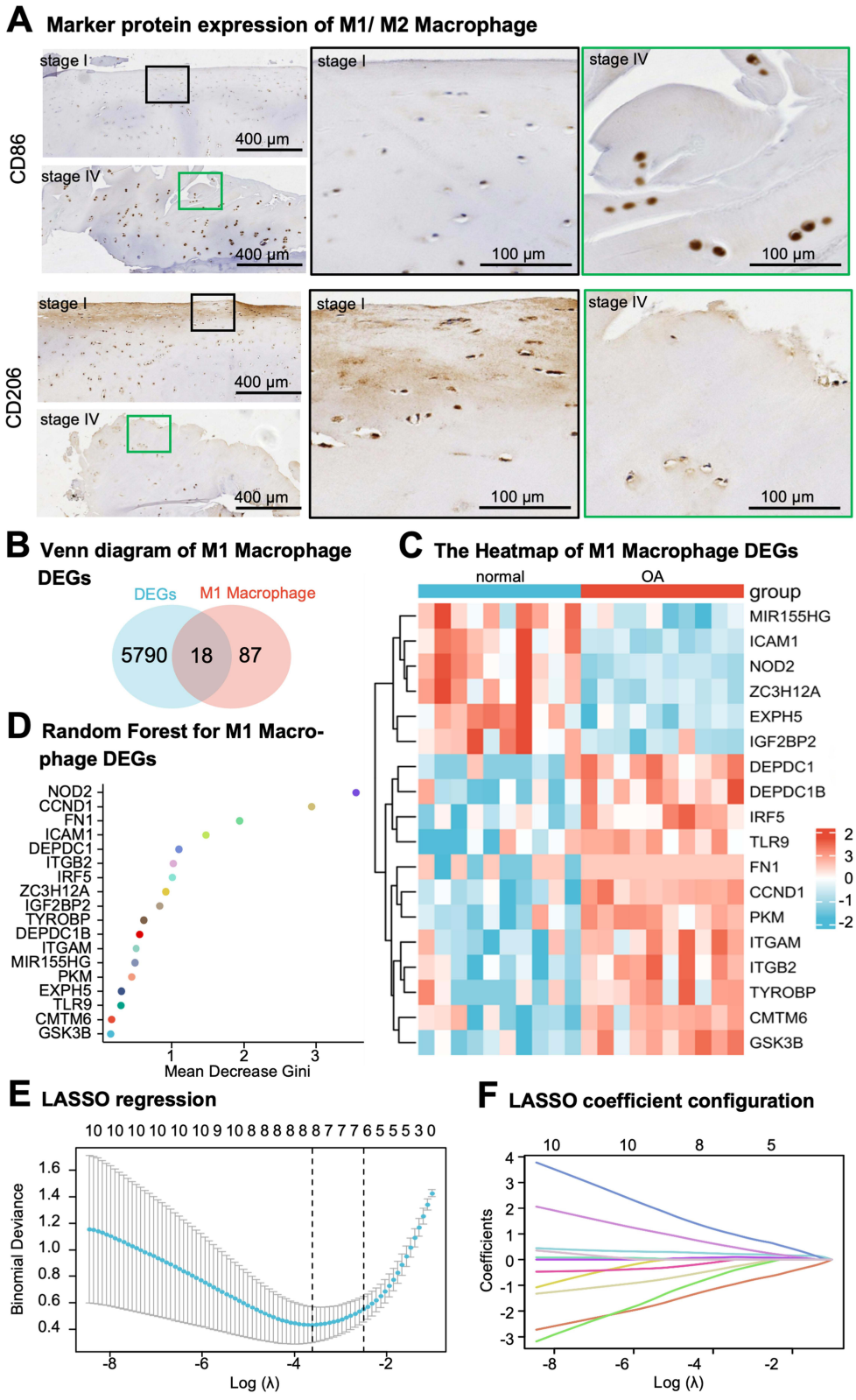

Figure 7 Machine learning-based identification of key genes mediating M1 macrophage infiltration in osteoarthritic cartilage. (**A**) Immunohistochemical staining of M1/M2 macrophage polarization markers. The higher-magnification images with black and green borders on the right correspond to the areas enclosed by the black and green rectangles in the lower-magnification image on the left. (**B**) Venn diagram screening M1 macrophage-associated genes in the GSE114007 dataset. (**C**) Heatmap of M1 macrophage-associated differentially expressed genes. (**D**) Bubble plot of importance scores for M1 macrophage-associated DEGs. (**E** and **F**) LASSO regression-based screening of M1 macrophage-associated DEGs.

https://doi.org/10.2147/JIR.S568766

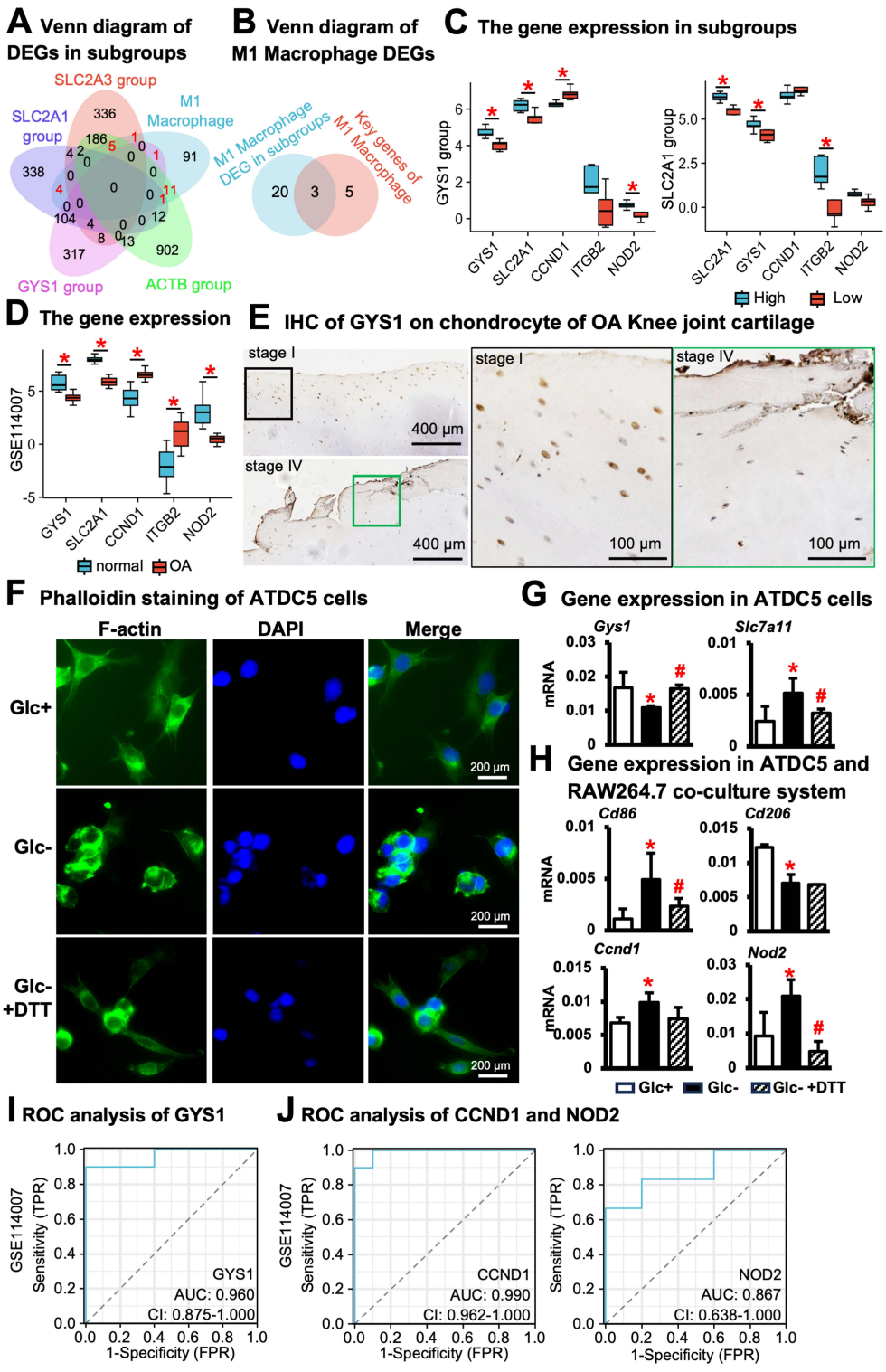

Figure 8 GYS1-Mediated Disulfidptosis Drives M1 Macrophage Polarization in the Osteoarthritic Niche. (**A**) Volcano plot of DEGs in GSE114007 re-stratified by four disulfidptosis-associated genes. (**B**) Venn diagram intersecting DEGs from four subgroups with M1 macrophage-associated genes, yielding 23 overlapping DEGs. (**C**) Intersection of 23 DEGs with M1 macrophage hub genes identifies 3 core DEGs. (**D**) Expression patterns of core DEGs across re-stratified subgroups. (**E**) Immunohistochemical staining of GYS1 protein. The higher-magnification images with black and green borders on the right correspond to the areas enclosed by the black and green rectangles in the lower-magnification image on the left. (**F**) Phalloidin staining of ATDC5 cells. (**G**) RT-qPCR assay for disulfidptosis-related gene expression in ATDC5 cells. (**H**) RT-qPCR assay for macrophage polarization and target gene expression in the ATDC5 and RAW264.7 co-culture system. (**I**) ROC analysis of GYS1. (**J**) ROC analysis of CCND1 and NOD2. Data were expressed as the mean ± standard deviation (SD). *p < 0.05 vs High group by *t*-test for panels (**C**). *p < 0.05 vs normal by *t*-test for panels (**D**). *p < 0.05 vs Glu-, #p < 0.05 vs Glu+ by One-Way ANOVA for panels (**G** and **H**).

https://doi.org/10.2147/JIR.S568766

ROC Analysis Validates the Diagnostic Potential of Disulfidptosis and M1-Related Gene Signatures

GYS1 is a key rate-limiting enzyme in glycogen synthesis. It is responsible for making a protein called glycogen synthase, which binds glucose molecules into strings to form the familiar glycogen.[32,33] It is the body's way of storing glucose. SLC2A1 is a member of the SLC2A family and is primarily responsible for the transmembrane transport of glucose, which is independent of insulin and therefore essential in maintaining basal glucose metabolism levels.[34] The expression of SLC2A1 and GYS1 is reduced in the severely damaged area of articular cartilage in OA patients, thus creating glucose starvation conditions, which is a prerequisite for inducing disulfidptosis of chondrocytes with high expression of SLC7A11 in the severely damaged area. We detected the expression of these two genes in different grades of articular cartilage tissues by immunohistochemistry, and found that GLUT1 protein encoded by *SLC2A1* showed no statistically significant overall change (Figure S5B), a trend which may be attributed to underlying metabolic disorders and also reflects the severity of OA progression. However, the expression of Glycogen Synthase protein encoded by *GYS1* is reduced at the injury site in region IV, which is consistent with gene expression changes (Figure 8E and S5B).

Therefore, we conducted in vitro cell experiments for validation. Phalloidin staining revealed that chondrocyte ATDC5 cells under glucose starvation underwent significant morphological changes, characterized by cell shrinkage and F-actin contraction, along with decreased expression of the marker gene *Gys1* and increased expression of *Slc7a11* (Figure 8F and G). Treatment with 0.5 mM of the strong reducing agent DTT (which effectively inhibits disulfidptosis)[29] impeded the morphological alterations in ATDC5 cells under glucose starvation, substantially restoring the cytoskeleton and reversing the expression of *Gys1* and *Slc7a11* genes (Figure 8F and G).

Following 12 hours of glucose starvation, ATDC5 cells were switched to normal culture medium and co-cultured with RAW264.7 macrophages. RT-qPCR analysis showed a significant increase in the expression of the M1 macrophage polarization marker gene *Cd86* and a decrease in the M2 polarization marker gene *Cd206* (Figure 8H), demonstrating that disulfidptosis in ATDC5 cells may induce macrophage polarization toward the M1 phenotype. Furthermore, the expression of the target gene *Ccnd1* increased, consistent with the phenotype observed in clinical OA cartilage tissues. Combined DTT treatment reversed the glucose starvation-induced increase in *Cd86* and showed a trend toward reversing the change in *Ccnd1* expression, suggesting that the decrease in *Gys1* in ATDC5 cells under glucose starvation, which promotes M1 macrophage polarization, may be associated with alterations in the *Ccnd1* gene. Although the expression of *Nod2* was opposite to the bioinformatics analysis results, this discrepancy may be attributed to the relatively short 12-hour in vitro treatment, which may not fully replicate the chronic processes occurring in vivo in OA. Subsequent research should consider the differences between acute stress models in vitro and chronic disease states in vivo, and explore glucose starvation treatment methods that better simulate the chronic in vivo process.

In addition, we analyzed the accuracy of *GYS1* genes in predicting OA outcome through diagnostic ROC, *GYS1* exhibited an AUC of 0.96 in the GSE114007 dataset (Figure 8I), indicating outstanding discriminative capacity for OA. The M1 macrophage-related genes *CCND1* and *NOD2*—regulated by *GYS1*—also showed high diagnostic accuracy, with AUCs of 0.99 and 0.867, respectively (Figure 8J), supporting their potential as biomarkers for OA progression.

Discussion

Degenerative Osteoarthritis (OA) is an age-related disease of progressive articular cartilage destruction that affects more than 300 million patients. Current treatments still have limitations in alleviating symptoms and improving patients' quality of life. In this study, we investigated the relationship between disulfidptosis, glucose metabolism and immune infiltration in the pathological mechanism of OA, and analyzed its potential therapeutic targets. Disulfidptosis is caused by increased cysteine transport and glutathione synthesis in SLC7A11 hyper expressing cells, which leads to abnormal accumulation of protein disulfide bonds and ultimately disulfidptosis in glucose deficient conditions. Analysis of sequencing data showed that the expression of genes related to glucose metabolic transport process was decreased in the knee cartilage tissue of OA patients. Immunohistochemistry of knee cartilage also showed that SLC7A11 was highly expressed in chondrocytes in the severely injured area of 75% of OA patients, indicating potential disulfidptosis in local chondrocytes. Additionally, integrated bioinformatics and immunohistochemical analyses revealed significant M1

macrophage infiltration in OA patients. Critically, the disulfidptosis-associated DEG *GSY1* was found to modulate the expression of M1 phenotype-defining genes *CCND1* and *NOD2*, thereby regulating macrophage immune infiltration. This mechanistic insight provides a novel diagnostic and therapeutic angle for early-stage osteoarthritis management.

SLC7A11 is known for its ability to inhibit iron deposition by promoting cysteine uptake and synthesizing glutathione, thereby combating lipid peroxidation.[35] However, new evidence reveals the dual role of SLC7A11 in cell fate. It is crucial that its role in disulfide induced ptosis is different in mechanism, even opposite to its role in iron induced ptosis.[4] The high expression level of SLC7A11 is the triggering event in bipedal ptosis. In the absence of glucose, overexpression of SLC7A11 can lead to excessive cysteine input, which cannot be fully reduced due to insufficient NADPH. This leads to catastrophic accumulation of intracellular disulfides and subsequent collapse of the actin cytoskeleton, a pathway completely independent of iron dependent lipid peroxidation.[4] In our study of OA, we observed a significant upregulation of SLC7A11, which is consistent with the prerequisite for the onset of disulfide ptosis, rather than the inhibitory feature of iron ptosis. In addition, its expression is more strongly correlated with other disulfide dependent genes such as RPN1 and CAPZB than with established iron dependent markers such as PTGS2 and ACSL4.[36] Therefore, while we acknowledge the well-known role of SLC7A11 in iron deposition, we propose that in the specific pathological context of OA - marked by metabolic stress and our identified gene expression patterns - SLC7A11 can serve as a more relevant biomarker for indicating susceptibility to disulfide deposition.

The primary innovation of this study lies in the integrated validation of disulfidptosis occurrence within OA articular cartilage, combining clinical specimen analysis with systematic bioinformatics exploration. While emerging studies have begun to associate disulfidptosis with OA through bioinformatics predictions,[13,15] direct evidence from patient-derived cartilage samples and mechanistic dissection within the chondrocyte-immune microenvironment remained limited. Our high-throughput sequencing analysis of clinical OA cartilage not only confirmed significant differential expression of disulfidptosis-related genes but also, through subsequent experimental validation, demonstrated the functional occurrence of disulfidptosis in OA chondrocytes. Sequencing data analysis showed that genes including *SLC2A1, SLC2A3, OXSM, GYS1*, and *SLC3A2*—all critically involved in glucose metabolism—were downregulated, indicating an impaired glucose transport state in OA chondrocytes. Additionally, differentially expressed genes such as *CAPZB, MYH9* and *ACTB*, which are associated with cytoskeletal reorganization, directly correlate with core features of disulfidptosis (actin disulfide crosslinking and cytoskeletal collapse), further supporting the occurrence of disulfidptosis in chondrocytes. Moreover, we detected elevated SLC7A11 expression in severely damaged areas of 75% of OA patients, a prerequisite for disulfidptosis. These finding challenges traditional understanding of OA pathogenesis and provides a crucial foundation for exploring novel therapeutic targets.

Macrophage immune infiltration plays a critical role in OA progression by modulating local inflammatory responses.[37,38] Our data analysis revealed significantly altered macrophage infiltration in OA patients, suggesting its pivotal involvement in disease advancement. While M1 macrophages secrete pro-inflammatory cytokines that accelerate OA pathogenesis, M2 macrophages exert beneficial effects through tissue repair and anti-inflammatory functions.[39] Notably, M1 macrophages extensively infiltrate the OA synovium, releasing TNF-α, IL-1β and other pro-inflammatory mediators that directly degrade cartilage matrix while simultaneously inducing synovial fibroblasts to produce additional inflammatory factors.[40] Our key finding establishes a robust association between M1 macrophage infiltration and disulfidptosis-related gene expression, with reduced *GYS1* expression effectively mediating the expression of macrophage-related key genes *CCND1* and *NOD*2. Specifically: Elevated CCND1 (Cyclin D1) correlates with enhanced inflammation via M1-driven cytokine release and stimulation of neighboring cell proliferation. Decreased NOD2 expression (a crucial pattern recognition receptor) compromises cellular recognition of endogenous stimuli, triggering localized inflammatory imbalance. This constitutes our second major research innovation: the discovery of molecular crosstalk between disulfidptosis and the OA immune microenvironment through the GYS1-CCND1/NOD2 regulatory axis.

Our transcriptomic data revealed downregulation of multiple genes involved in glucose metabolism and transport in osteoarthritic cartilage. KEGG pathway analysis further demonstrated significant enrichment of disulfidptosis-related DEGs in glucose metabolism and insulin signaling pathways. These findings collectively indicate a hypoglycemic microenvironment conducive to disulfidptosis. Immunohistochemical validation at the protein level confirmed reduced

GYS1 expression in the severely damaged stage IV of OA cartilage. Although the expression of the glucose transporter GLUT1 (encoded by *SLC2A1*) showed no statistically significant difference, this overall dysregulation of metabolic gene expression likely reflects a state of glucose metabolic imbalance, which may disrupt redox homeostasis and facilitate disulfidptosis.

While this study provides novel insights into the interrelationship among disulfidptosis, immune infiltration, and glucose metabolism in OA pathogenesis, several limitations warrant consideration. Specifically, although our in vitro co-culture system provides initial functional validation, the mutual regulatory mechanisms between disulfidptotic chondrocytes and macrophages remain incompletely characterized. To comprehensively elucidate the causal relationships and translational relevance, future work should incorporate: 1) Advanced mechanistic studies to dissect the reciprocal signaling pathways between disulfidptotic chondrocytes and macrophages, including potential feedback loops; 2) Genetic perturbation models (eg, chondrocyte-specific GYS1-KO mice) to assess the in vivo role of disulfidptosis in OA progression and immune infiltration; 3) Metabolic flux analysis to quantify how glucose starvation triggers the disulfidptosis-immunity axis within the joint microenvironment, such as by monitoring changes in NADPH levels, cystine accumulation, or redox balance. Therapeutically, our findings on the disulfidptosis-immunity axis suggest novel strategies for OA treatment. For example, redox-modulating compounds like carboxymethyl-chitosan (CM-C)—known for its antioxidant and anti-inflammatory effects in joints—could be explored as potential therapies targeting this axis.[41] Future studies should test whether such interventions mitigate disulfidptosis-driven immune dysregulation and OA progression.

In summary, this study demonstrates that altered expression of disulfidptosis-related genes in osteoarthritic cartilage is closely associated with immune cell infiltration, providing new insights into the pathogenesis of osteoarthritis. Our findings highlight the functional significance of these genes in modulating chondrocyte-immune crosstalk, suggesting that targeting disulfidptosis may represent a promising therapeutic strategy for osteoarthritis. These results establish a foundation for further mechanistic investigation and potential clinical translation, underscoring the importance of disulfidptosis in OA progression.

Conclusion

Disulfidptosis in chondrocytes is closely linked to M1 macrophage immune infiltration and may serve as a mechanistic driver of OA progression. Mechanism genes such as GYS1/CCND1/NOD2 show strong diagnostic potential and may represent novel biomarkers and therapeutic targets for OA prevention and treatment.

Data Sharing Statement

All data generated for this study are available from the corresponding authors upon reasonable request.

Ethics Approval and Consent to Participate

The study protocol was approved by the Ethics Committee of Yongchuan Hospital Affiliated to Chongqing Medical University with protocol number 2024EC0074 and Chinese Clinical Registry number ChiCTR2500097743. Informed consent was obtained from all subjects involved in the study.

Author Contributions

YM.Q.: Conceptualization, Methodology, Formal analysis, Writing – original draft, Writing – review & editing. YJ.L.: Conceptualization, Methodology, Formal analysis, Writing – original draft, Writing – review & editing. Q.S.: Methodology, Investigation, Formal analysis, Writing – original draft, Writing – review & editing. ZH.W.: Methodology, Investigation, Formal analysis, Writing – original draft, Writing – review & editing. GH.S.: Methodology, Investigation, Formal analysis, Writing – review & editing. MF.Y.: Investigation, Writing – review & editing. X.H.: Investigation, Writing – review & editing. SH.D.: Investigation, Writing – review & editing. XY.Z.: Investigation, Formal analysis, Writing – review & editing. R.G.: Investigation, Formal analysis, Writing – review & editing. H.Z.: Investigation, Writing – review & editing. YN.Z.: Investigation, Formal analysis, Writing – review & editing. All authors made a significant contribution to the work reported, whether that is in the conception, study design,

execution, acquisition of data, analysis and interpretation, or in all these areas; took part in drafting, revising or critically reviewing the article; gave final approval of the version to be published; have agreed on the journal to which the article has been submitted; and agree to be accountable for all aspects of the work.

Funding

This research was funded by National funded Postdoctoral Researcher Program of China GZC20233350 (YJ.L.); Chongqing Municipal Special Program for Technological Innovation and Application Development - Key Project CSTB2022TIAD-KPX0172 (GH.S.); Chongqing Natural Science Foundation -General Project CSTB2024NSCQ-MSX0145 (YJ.L.); Research Project Funded by the Affiliated Yongchuan Hospital of Chongqing Medical University YJSJ202137 (GH.S.), YJSJ202134 (ZH.W.), YJSJ202138 (YM.Q.) and YJJL2024006 (YJ.L.). Chongqing Postgraduate Research and Innovation Project CYB19167 (YN.Z.).

Disclosure

These authors declare to have no competing financial interests, Including the order of co-authors and corresponding authors.

References

1. Yao Q, Wu X, Tao C, et al. Osteoarthritis: pathogenic signaling pathways and therapeutic targets. *Signal Transduct Target Ther*. 2023;8(1):56. doi:10.1038/s41392-023-01330-w
2. Fusco M, Skaper SD, Coaccioli S, Varrassi G, Paladini A. Degenerative joint diseases and neuroinflammation. *Pain Pract*. 2017;17(4):522–532. doi:10.1111/papr.12551
3. Qian W, Ji R, Ye Q, et al. Inotodiol ameliorates the progression of osteoarthritis: an in vitro and in vivo study. *Drug Res*. 2023;73(9):506–512. doi:10.1055/a-2176-4098
4. Liu X, Nie L, Zhang Y, et al. Actin cytoskeleton vulnerability to disulfide stress mediates disulfidptosis. *Nat Cell Biol*. 2023;25(3):404–414. doi:10.1038/s41556-023-01091-2
5. Zhu Y, Kong L, Han T, Yan Q, Liu J. Machine learning identification and immune infiltration of disulfidptosis-related Alzheimer's disease molecular subtypes. *Immun Inflamm Dis*. 2023;11(10):e1037. doi:10.1002/iid3.1037
6. Ma S, Wang D, Xie D. Identification of disulfidptosis-related genes and subgroups in Alzheimer's disease. *Front Aging Neurosci*. 2023;15:1236490. doi:10.3389/fnagi.2023.1236490
7. Wu Q, Liu SP, Liu C, Chen X, Zhou H, Zhao H. Disulfidoptosis as a novel mechanism of neuronal death: insights from Creutzfeldt-Jakob disease. *World Neurosurg*. 2024;191:e92–e106. doi:10.1016/j.wneu.2024.08.070
8. Liu Y, Sun Y, Chen A, et al. Involvement of disulfidptosis in the pathophysiology of autism spectrum disorder. *Life Sci*. 2025;369:123531. doi:10.1016/j.lfs.2025.123531
9. Chen Y, Xue W, Zhang Y, Gao Y, Wang Y. A novel disulfidptosis-related immune checkpoint genes signature: forecasting the prognosis of hepatocellular carcinoma. *J Cancer Res Clin Oncol*. 2023;149(14):12843–12854. doi:10.1007/s00432-023-05076-4
10. Yu X, Guo Z, Fang Z, et al. Identification and validation of disulfidptosis-associated molecular clusters in non-alcoholic fatty liver disease. *Front Genet*. 2023;14:1251999. doi:10.3389/fgene.2023.1251999
11. Chen X, Wang Z, Wu Y, Lan Y, Li Y. Typing and modeling of hepatocellular carcinoma based on disulfidptosis-related amino acid metabolism genes for predicting prognosis and guiding individualized treatment. *Front Oncol*. 2023;13:1204335. doi:10.3389/fonc.2023.1204335
12. Zheng S, Li Y, Yin L, Lu M. Identification of sulfur metabolism-related gene signature in osteoarthritis and TM9SF2's sustenance effect on M2 macrophages' phagocytic activity. *J Orthop Surg Res*. 2024;19(1):62. doi:10.1186/s13018-023-04384-2
13. Wei M, Shi X, Tang W, Lv Q, Wu Y, Xu Y. Identification of a novel disulfidptosis-related gene signature in osteoarthritis using bioinformatics analysis and experimental validation. *Sci Rep*. 2025;15(1):1339. doi:10.1038/s41598-025-85569-z
14. Hu K, Ou Y, Xiao L, et al. Identification and construction of a disulfidptosis-mediated diagnostic model and associated immune microenvironment of osteoarthritis from the perspective of PPPM. *J Inflamm Res*. 2024;17:3753–3770. doi:10.2147/jir.S462179
15. Cao S, Wei Y, Yue Y, et al. Bioinformatics identification and experimental verification of disulfidptosis-related genes in the progression of osteoarthritis. *Biomedicines*. 2024;12(8):1840. doi:10.3390/biomedicines12081840
16. Yura S, Harada S, Kobayashi K. Diagnostic accuracy on magnetic resonance imaging for the diagnosis of osteoarthritis of the temporomandibular joint. *J Clin Diagn Res*. 2015;9(7):Zc95–7. doi:10.7860/jcdr/2015/12302.6260
17. López de Figueroa P, Lotz MK, Blanco FJ, Caramés B. Autophagy activation and protection from mitochondrial dysfunction in human chondrocytes. *Arthritis Rheumatol*. 2015;67(4):966–976. doi:10.1002/art.39025
18. Liu Z, Sun L, Zhu W, et al. Disulfidptosis signature predicts immune microenvironment and prognosis of gastric cancer. *Biol Direct*. 2024;19(1):65. doi:10.1186/s13062-024-00518-6
19. Xu K, Li D, Ji K, et al. Disulfidptosis-associated LncRNA signature predicts prognosis and immune response in kidney renal clear cell carcinoma. *Biol Direct*. 2024;19(1):71. doi:10.1186/s13062-024-00517-7
20. Zhu Y, Wang X, Feng L, et al. Intermetallics triggering pyroptosis and disulfidptosis in cancer cells promote anti-tumor immunity. *Nat Commun*. 2024;15(1):8696. doi:10.1038/s41467-024-53135-2
21. Tan X, Zhang N, Zhang G, et al. Exploring the diagnostic and immune infiltration roles of disulfidptosis related genes in pulmonary hypertension. *Respir Res*. 2024;25(1):365. doi:10.1186/s12931-024-02978-w

22. Jiang T, Su S, Tian R, et al. Immunoregulatory orchestrations in osteoarthritis and mesenchymal stromal cells for therapy. *J Orthop Translat*. 2025;55:38–54. doi:10.1016/j.jot.2025.08.009
23. Wan J, Shi JH, Shi M, et al. Lactate dehydrogenase B facilitates disulfidptosis and exhaustion of tumour-infiltrating CD8(+) T cells. *Nat Cell Biol*. 2025;27(6):972–982. doi:10.1038/s41556-025-01673-2
24. Shi M, Wang J, Xiao Y, et al. Glycogen metabolism and rheumatoid arthritis: the role of glycogen synthase 1 in regulation of synovial inflammation via blocking AMP-activated protein kinase activation. *Front Immunol*. 2018;9:1714. doi:10.3389/fimmu.2018.01714
25. Wu CY, Liu Z, Luo WM, et al. Downregulation of DIP2B as a prognostic marker inhibited cancer proliferation and migration and was associated with immune infiltration in lung adenocarcinoma via CCND1 and MMP2. *Heliyon*. 2024;10(12):e32025. doi:10.1016/j.heliyon.2024.e32025
26. Zhang Q, Ji Q, Wang X, et al. SOX9 is a regulator of ADAMTSs-induced cartilage degeneration at the early stage of human osteoarthritis. *Osteoarthritis Cartilage*. 2015;23(12):2259–2268. doi:10.1016/j.joca.2015.06.014
27. Wang X, Ma Y, Chen J, et al. A novel decellularized matrix of Wnt signaling-activated osteocytes accelerates the repair of critical-sized parietal bone defects with osteoclastogenesis, angiogenesis, and neurogenesis. *Bioact Mater*. 2023;21:110–128. doi:10.1016/j.bioactmat.2022.07.017
28. Bindea G, Mlecnik B, Tosolini M, et al. Spatiotemporal dynamics of intratumoral immune cells reveal the immune landscape in human cancer. *Immunity*. 2013;39(4):782–795. doi:10.1016/j.immuni.2013.10.003
29. Yao H, Liu P, Yao L, Li X. Establishment of disulfidptosis-related LncRNA signature as biomarkers in colon adenocarcinoma. *Cancer Cell Int*. 2024;24(1):183. doi:10.1186/s12935-024-03374-6
30. Liu Y, Zhao L, Li M, et al. Osteocytes produces RANKL via Wnt-TGFβ signaling axis for osteoclastogenesis. *Int J Biol Sci*. 2025;21(13):5821–5841. doi:10.7150/ijbs.117481
31. Blom AB, van Lent PL, Libregts S, et al. Crucial role of macrophages in matrix metalloproteinase-mediated cartilage destruction during experimental osteoarthritis: involvement of matrix metalloproteinase 3. *Arthritis Rheum*. 2007;56(1):147–157. doi:10.1002/art.22337
32. Pederson BA, Schroeder JM, Parker GE, Smith MW, DePaoli-Roach AA, Roach PJ. Glucose metabolism in mice lacking muscle glycogen synthase. *Diabetes*. 2005;54(12):3466–3473. doi:10.2337/diabetes.54.12.3466
33. Xirouchaki CE, Mangiafico SP, Bate K, et al. Impaired glucose metabolism and exercise capacity with muscle-specific glycogen synthase 1 (gys1) deletion in adult mice. *Mol Metab*. 2016;5(3):221–232. doi:10.1016/j.molmet.2016.01.004
34. Arhin SK, Zhao J, Ji X, et al. Multiple facilitated glucose transporters SLC2As are required for normal mouse preimplantation embryo development. *Am J Transl Res*. 2019;11(6):3412–3425.
35. Koppula P, Zhuang L, Gan B. Cystine transporter SLC7A11/xCT in cancer: ferroptosis, nutrient dependency, and cancer therapy. *Protein Cell*. 2021;12(8):599–620. doi:10.1007/s13238-020-00789-5
36. Qiu H, Liu J, Shao N, et al. SLC7A11 as a bridge between ferroptosis and disulfidptosis: a promising target for tumor treatment. *Cell Commun Signal*. 2025;23(1):460. doi:10.1186/s12964-025-02447-x
37. Lopes EBP, Filiberti A, Husain SA, Humphrey MB. Immune Contributions to Osteoarthritis. *Curr Osteoporos Rep*. 2017;15(6):593–600. doi:10.1007/s11914-017-0411-y
38. Gaigeard N, Cardon A, Le Goff B, Guicheux J, Boutet MA. Unveiling the macrophage dynamics in osteoarthritic joints: from inflammation to therapeutic strategies. *Drug Discov Today*. 2024;29(11):104187. doi:10.1016/j.drudis.2024.104187
39. Wu CL, Harasymowicz NS, Klimak MA, Collins KH, Guilak F. The role of macrophages in osteoarthritis and cartilage repair. *Osteoarthritis Cartilage*. 2020;28(5):544–554. doi:10.1016/j.joca.2019.12.007
40. Zhang H, Cai D, Bai X. Macrophages regulate the progression of osteoarthritis. *Osteoarthritis Cartilage*. 2020;28(5):555–561. doi:10.1016/j.joca.2020.01.007
41. Manocchio N, Pirri C, Ljoka C, et al. Long-term efficacy of carboxymethyl-chitosan in advanced knee osteoarthritis: a twelve-month follow-up study on non-responders to hyaluronic acid. *Biomedicines*. 2025;13(2). doi:10.3390/biomedicines13020270